Kinetic Studies on the Inhibition of Isopeptidase T by Ubiquitin Aldehyde

Francesco Melandri,[‡] Louis Grenier,[‡] Louis Plamondon,[‡] W. Phillip Huskey,[§] and Ross L. Stein*[,‡]

ProScript, Inc., 38 Sidney Street, Cambridge, Massachusetts 02139, and Rutgers, The State University of New Jersey, Department of Chemistry (Newark Campus), Newark, New Jersey 07102

Received May 31, 1996; Revised Manuscript Received July 17, 1996[⊗]

ABSTRACT: Isopeptidase T (IPaseT) can hydrolyze isopeptide bonds of polyubiquitin (polyUb) chains, simple C-terminal derivatives of Ub, and certain peptides. We recently reported that IPaseT is regulated by ubiquitin (Ub); while submicromolar Ub activates, higher concentrations inhibit this enzyme [Stein et al. (1995) *Biochemistry 34*, 12616]. To explain these observations, we proposed a model for IPaseT involving two binding sites for Ub. According to the model, the two sites are adjacent to one another and are the extended active site that binds two Ub moieties of a polyUb chain. The "activation site" binds the Ub that donates Lys to the isopeptide bond. The "inhibition site" is adjacent and binds the Ub that donates the C-terminal Gly to the isopeptide bond. We now report that the interaction of IPaseT with the C-terminal aldehyde of Ub (Ub-H) is also modulated by Ub. In the absence of Ub, Ub-H inhibits IPaseT with a K_i of 2.3 nM, while at 0.6 μM Ub, where the "activation site" is occupied, K_i is less than 0.1 nM. At high Ub concentrations, where both the "activation" and "inhibition" sites are occupied, IPaseT cannot bind Ub-H. We also determined the kinetics of inhibition of IPaseT by Ub-H. In the absence of Ub, a two-step mechanism is followed. In the first step, Ub-H slowly combines with IPaseT to form a relatively weak complex ($K_1 = 260$ nM) that slowly isomerizes to the final, stable complex that accumulates in the steady-state ($k_2 = 2 \times 10^{-3}$ s^{-1}; $k_{-2} = 0.02 \times 10^{-3}$ s^{-1}). In contrast, Ub-activated IPaseT is inhibited by Ub-H through a three-step process. In the first step, Ub-H rapidly combines with IPaseT to form a complex ($K_1 = 10$ nM) that slowly isomerizes to a second, more stable complex ($k_2 = 18 \times 10^{-3}$ s^{-1}; $k_{-2} = 1.5 \times 10^{-3}$ s^{-1}). In the third step, the second complex converts to the final complex ($k_3 = 1.5 \times 10^{-3}$ s^{-1}; $k_{-3} < 0.2 \times 10^{-3}$ s^{-1}). To unify the results of this study with our previous results on catalysis, we propose that binding of Ub either to catalytic transition states or to tetrahedral inhibition intermediates liberates more free energy than binding of Ub to the reactant state of IPaseT and that IPaseT can utilize this binding energy to stabilize both of these tetrahedral species. The overall effect is a Ub-induced increase in catalytic efficiency or inhibitory potency.

The ubiquitin−proteasome pathway of protein degradation is the principle mechanism for intracellular protein catabolism and has both house-keeping roles and roles in the turnover of many regulatory proteins (Ciechanover, 1994; Finley & Chau, 1991; Goldberg & Mitch, 1996; Hochstrasser, 1995; Wilkinson, 1995). Proteins that are destined to be degraded through the ubiquitin-proteasome pathway are first covalently tagged with a molecule of ubiquitin, a 8.6 kDa heat-stable protein. This tagging reaction involves three sequential enzyme-catalyzed steps that ultimately ligates the C-terminal Gly of Ub[1] onto ϵ-amines of Lys residues on the substrate protein. A polyUb chain is then elaborated on the protein through the ligation of additional monomers of Ub to the first Ub in successive rounds of ubiquitination. These Ub molecules are added to specific Lys residues of the proximal Ub of the propagating polyUb chain. Proteins with long polyUb chains can be recognized by the 26S proteasome complex which first cleaves off the polyUb chains and then degrades the protein substrate to small peptides (Hadar et al., 1992; Wilkinson, 1995; Wilkinson et al., 1995). Alternately, the poly-ubiquitinated protein will be subject to the action of isopeptidases, enzymes that hydrolyze isopeptide bonds and serve to cleave off Ub and regenerate intact protein.

Isopeptidases are members of a large family of ubiquitin C-terminal hydrolases (Mayer & Wilkinson, 1989; Stein et al., 1995; Wilkinson, 1995; Wilkinson et al., 1995). While these enzymes differ widely in their size and role in cellular physiology, they all hydrolyze their substrates through a common mechanism involving nucleophilic attack of an active site Cys residue and are all susceptible to inhibition by ubiquitin C-terminal aldehyde (Ub-H), a synthetic analog of Ub (Hershko & Rose, 1987; Pickart & Rose, 1985, 1986; Wilkinson et al., 1986). Ub-H is thought to inhibit UCH's through a mechanism that is analogous to the mechanism of inhibition of cysteine proteases by peptide aldehydes (Lewis & Wofenden, 1977a,b) involving the reversible formation of a hemithioacetal.

One member of the UCH family is isopeptidase T (Chen & Pickart, 1990; Hadar et al., 1992; Stein et al., 1995; Wilkinson, 1995; Wilkinson et al., 1995). This enzyme is thought to trim Ub monomers from the C-termini of polyUb chains (Hadar et al., 1992; Wilkinson, 1995; Wilkinson et al., 1995) and thus may play a role in the regulation of protein

* To whom correspondence should be addressed.
[‡] ProScript, Inc.
[§] Rutgers, The State University of New Jersey.
[⊗] Abstract published in *Advance ACS Abstracts,* September 1, 1996.
[1] Abbreviations: AMC, aminomethylcoumarin; DTT, dithiothreitol; FI, fluorescence intensity; IPaseT, isopeptidase T; polyUb, polyubiquitin chains formed through isopeptide linkages of Gly^{76} of one Ub and the ϵ-amine of Lys^{48} of another Ub; Ub, ubiquitin; Ub-H, ubiquitin aldehyde; UCH, ubiquitin C-terminal hydrolases; K_i, observed mechanism-independent steady-state dissociation constant for an enzyme−inhibitor complex.

S0006-2960(96)01293-7 CCC: $12.00

turnover through the ubiquitin−proteasome pathway by preventing the buildup of free polyUb chains which are known to inhibit the 26S proteasome complex (Hadar et al., 1992). Previously, we reported a series of low-molecular weight substrates for IPaseT that are appropriate for detailed kinetic and mechanistic studies (Stein et al., 1995). These substrates are peptide-AMC's based on the C-terminus of Ub and were shown to form the basis of sensitive assays for IPaseT. In the course of these studies, we also found that Ub can modulate the kinetics of these reactions.

In this paper, we extend our studies of IPaseT and report on the inhibition of IPaseT by Ub-H. This is the first detailed kinetic investigation of the inhibition of an UCH by Ub-H. We find that Ub-H is a slow-binding inhibitor and, furthermore, like the peptidase activity of IPaseT, the kinetics of inhibition are modulated by Ub.

EXPERIMENTAL PROCEDURES

General. Buffer salts were purchased from Sigma Chemical Co. Bovine trypsin was from Sigma, and yeast carboxypeptidase Y was from Calbiochem. Peptide substrates were custom synthesized by Enzyme System Products (Dublin, CA) at a purity greater than 95%. Isopeptidase T was prepared from rabbit reticulocytes as previously reported (Chen & Pickart, 1990; Stein et al., 1995).

Preparation of Ubiquitin Aldehyde. Ubiquitin C-terminal aldehyde was prepared either according to the method of Cohen (personal communication with R. Cohen) involving carboxypeptidase Y-catalyzed transpeptidation of 1-amino-2,3-propanediol (Aldrich) into Ub to form Ub-diol or according to the method of Dunten and Cohen (1989) involving trypsin-catalyzed transpeptidation of glycyl-3-amido-1,2-propanediol (see synthesis below) into Ub to form Ub-diol. Ub-diol is oxidized to the aldehyde with sodium periodate. Prior to oxidation, Ub-diol is purified by cation-exchange FPLC on a Mono S column (Pharmacia). Both preparations of Ub-H inhibit IPaseT with identical potencies and kinetic properties.

Chemical Synthesis of Glycyl-3-amido-1,2-propanediol. A solution of (±)-3-amino-1,2-propanediol (108 mmol) in 20 mL 1:1 THF/H_2O was treated with 1.1 equiv of di-*tert*-butyl dicarbonate and 2 equiv of triethylamine. The mixture was stirred at room temperature for 3 h, concentrated *in vacuo*, diluted with ethyl acetate, washed successively with water and brine, and then dried (Na_2SO_4). The BOC-protected aminodiol was then treated with 0.97 equiv of sodium hydride and 0.93 equiv of benzyl bromide in THF at −20 °C affording a mixture of mono- and dibenzylated diol which was carried through to the next step. The *tert*-butyloxycarbonyl group was removed with a 4 M solution of hydrochloric acid in 1,4-dioxane, and the salt was coupled to BOC-Gly-OH using excess 2-(1*H*-benzotriazol-1-yl)-1,1,3,3-tetramethyluronium tetrafluoroborate and diisopropylethylamine in anhydrous acetonitrile. The dark mixture was then diluted with ethyl acetate and washed successively with water, saturated aqueous sodium bicarbonate, and brine, and then dried ($MgSO_4$) and chromatographed (ethyl acetate, 230−400 mesh SiO_2). The benzyl groups were then removed by hydrogenation over Pearlman's catalyst [20% $Pd(OH)_2$/C] in methanol. The pure BOC-Gly-aminopropanediol was obtained by flash chromatography (230−400 mesh SiO_2) with 5% MeOH/$CHCl_3$ to 20% MeOH/$CHCl_3$ as eluant. The *tert*-butyloxycarbonyl group was finally removed by treating a solution of 3.32 g of the material in 25 mL of dichloromethane with a 1 M solution of hydrochloric acid in diethyl ether (1.94 equiv). Concentration *in vacuo* followed by washing with methanol/ethyl acetate afforded a gummy solid which was dissolved in water and lyophilized overnight to afford 2.03 g of desired Gly-aminopropanediol hydrochloride salt as a white gummy solid, homogeneous by HPLC and ^{1}H NMR.

Kinetic Methods: General. In a typical kinetic run, 2.00 mL of assay buffer (20 mM HEPES, 0.5 mM EDTA, pH 7.8, containing 1 mg of ovalbumin/mL and 10 mM DTT) was added to a 3 mL fluorescence cuvette, and the cuvette was placed in the jacketed cell holder of a Hitachi 2000 fluorescence spectrophotometer. Reaction temperature was maintained at 25.0 ± 0.02 °C by a circulating water bath. After the reaction solution had reached thermal equilibrium (∼5 min), 1−10 μL of the stock enzyme solution was added to the cuvette. The reaction solution was incubated an additional 30 min to allow DTT-mediated activation of IPaseT before the addition of 10 μL of substrate solution in DMSO. Reaction progress was monitored by the increase in fluorescence emission at 440 nm (λ_{ex} = 380 nm) that accompanies cleavage of AMC from peptide-AMC substrates. For each kinetic run, 200−1000 data points, corresponding to {time, FI} pairs, were collected by a microcomputer interfaced to the fluorescence spectrophotometer.

Kinetic Methods: Progress Curves for Inhibition of Isopeptidase T by Ubiquitin Aldehyde. In these experiments, linear progress curves for the steady-state hydrolysis of substrate are first collected for a time that is sufficient to allow determination of v_c, the control velocity in the absence of inhibitor. After these data have been collected, a small aliquot (∼10 μL) of Ub-H solution is added to the cuvette containing the reaction solution and the progress curve for time-dependent inhibition is then monitored. Analysis of these curves is described in detail below.

Kinetic Methods: Titration of Ubiquitin-Activated Isopeptidase T by Ubiquitin Aldehyde. To determine the steady-state dissociation constant for the inhibition of Ub-activated IPaseT by Ub-H, we conducted enzyme titration experiments in which residual activity is measured for enzyme reaction solutions in which $[I]_o \approx [E]_o \gg K_i$. Specifically, 2.00 mL reaction solutions containing 5 nM IPaseT, 0.6 μM Ub, and various concentrations of Ub-H were incubated at 25.0 ± 0.02 °C for 3 h. At this end of this time, residual IPaseT activity was measured with Z-Leu-Arg-Gly-Gly-AMC at a final concentration of 200 μM.

RESULTS

Kinetics of Inhibition of Isopeptidase T by Ubiquitin Aldehyde in the Absence of Ubiquitin. To characterize the kinetics of inhibition of IPaseT by Ub-H, we conducted experiments in which we monitored progress curves for the IPaseT-catalyzed hydrolysis of Z-Leu-Arg-Gly-Gly-AMC in the presence of Ub-H. An example of such a progress curve is shown in Figure 1 where we plot the data for an experiment in which [IPaseT] = 0.05 μM, [Z-Leu-Arg-Gly-Gly-AMC] = 400 μM, and [Ub-H] = 0.11 μM. In this and all other progress curves that we report, Ub-H was added to reaction solutions only after we had measured v_c, the control velocity in the absence of inhibitor. The shape of these

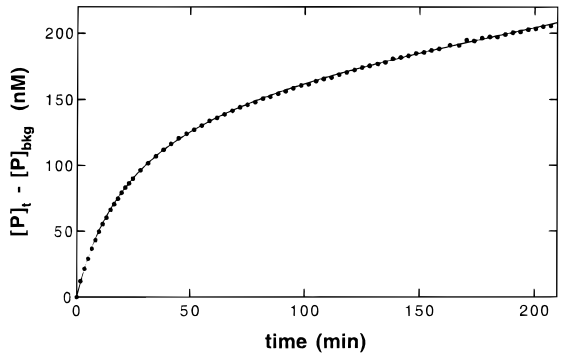

FIGURE 1: Progress curve for the inhibition of IPaseT by Ub-H. Fluorescence intensity ($\lambda_{em} = 440$ nm, $\lambda_{ex} = 380$ nm) was recorded as a function of time for the IPaseT-catalyzed hydrolysis of Z-Leu-Arg-Gly-Gly-AMC in the presence of Ub-H, converted to AMC concentration, and plotted here as the difference between product AMC concentration at any time, *t*, and the background AMC concentration. The reaction was conducted at 25 °C in a pH 7.8 assay buffer containing 20 mM HEPES, 0.5 mM EDTA, 1 mg of ovalbumin/mL, and 10 mM DTT. In this experiment, [IPaseT] = 0.05 μM, [Z-Leu-Arg-Gly-Gly-AMC] = 400 μM, [Ub-H] = 0.11 μM. The solid line through the data points was drawn with eq 2 and the best-fit parameters: $v_{i,o} = (119 \pm 1) \times 10^{-3}$ nM/s, $v_{i,s} = (6.0 \pm 0.1) \times 10^{-3}$ nM/s, $k_{obs} = (0.381 \pm 0.002) \times 10^{-3}$ s^{-1}, and $\gamma = 0.764 \pm 0.004$.

progress curves is characteristic of slow-binding inhibition (Szedlacsek & Duggleby, 1995; Williams & Morrison, 1979) where the initial velocity in the presence of inhibitor, $v_{i,o}$, decays to the final steady-state velocity, $v_{i,s}$, by a first-order rate process governed by k_{obs}. Typically, such curves can be fit to the expression of eq 1.

$$[P]_t = v_{i,s}t + \frac{v_{i,o} - v_{i,s}}{k_{obs}}(1 - e^{-k_{obs}t}) \quad (1)$$

However, in the experiment of Figure 1, inhibitor concentration was only twice the enzyme concentration and we therefore needed to use an expression that accounts for the decrease in inhibitor concentration that occurs as the enzyme:inhibitor complex forms (Szedlacsek & Duggleby, 1995; Williams & Morrison, 1979). This expression is given in eq 2

$$[P]_t = v_{i,s}t + \frac{(1-\gamma)(v_{i,o} - v_{i,s})}{\gamma k_{obs}} \ln\left(\frac{1 - \gamma e^{-k_{obs}t}}{1-\gamma}\right) \quad (2)$$

where

$$\gamma = \frac{[E]_o}{[I]_o}\left(1 - \frac{v_{i,s}}{v_{i,o}}\right)^2 \quad (3)$$

When the data of Figure 1 were fit to this expression, the following best-fit parameters were obtained: $v_{i,o} = (119 \pm 41) \times 10^{-3}$ nM/s, $v_{i,s} = (6.0 \pm 0.1) \times 10^{-3}$ nM/s, $k_{obs} = (3.81 \pm 0.02) \times 10^{-4}$ s^{-1}, and $\gamma = 0.764 \pm 0.004$. As part of this kinetic experiment, v_c was of course also determined and equals $(172 \pm 1) \times 10^{-3}$ nM/s (data not shown).

Note that v_c is greater than $v_{i,o}$. This suggests a mechanism in which enzyme rapidly combines with Ub-H to form the initial complex $(E:UbH)_1$ which then slowly isomerizes to $(E:UbH)_2$ (see Scheme 1, [Ub] = 0). The initial equilibrium step of this process is governed by K_{ei} which can be calculated according to the expression of eq 4.

$$K_{ei} = \frac{[\text{Ub-H}]}{\frac{v_c}{v_{i,o}} - 1} - \frac{v_{i,o}}{v_c}[E] \quad (4)$$

This expression takes into account the depletion of inhibitor that occurs as the enzyme:inhibitor complex forms (Greco & Hakala, 1979). From the experiment of Figure 1 we calculate $K_{ei} = 249$ nM and from triplicate experiments we calculate an average value of 262 ± 17 nM.

For this mechanism, k_{obs} is related to the mechanistic parameters as described in eq 5.

$$k_{obs} = k_{2,ei}\left(\frac{[\text{UbH}]}{K_{ei} + [\text{Ub-H}]}\right) \quad (5)$$

For Figure 1, we can use this expression to calculate that $k_{2,ei} = 1.24 \times 10^{-3}$ s^{-1}. Triplicate experiments provide $k_{2,ei} = (2.0 \pm 0.8) \times 10^{-3}$ s^{-1}.

K_{ei}*, the overall dissociation constant for the interaction of IPaseT and Ub-H at steady-state, can be calculated according to an expression that is analogous to that used for the calculation of K_{ei}.

$$K_{ei}^* = \frac{[\text{Ub-H}]}{\frac{v_c}{v_{i,s}} - 1} - \frac{v_{i,s}}{v_c}[E] \quad (6)$$

For Figure 1, we calculate $K_{ei}^* = 3.9$ nM. Triplicate experiments provide $K_{ei}^* = 2.3 \pm 1.2$ nM. Finally, we

Scheme 1: Mechanism of Slow-Binding Inhibition of Isopeptidase T by Uniquitin Aldehyde

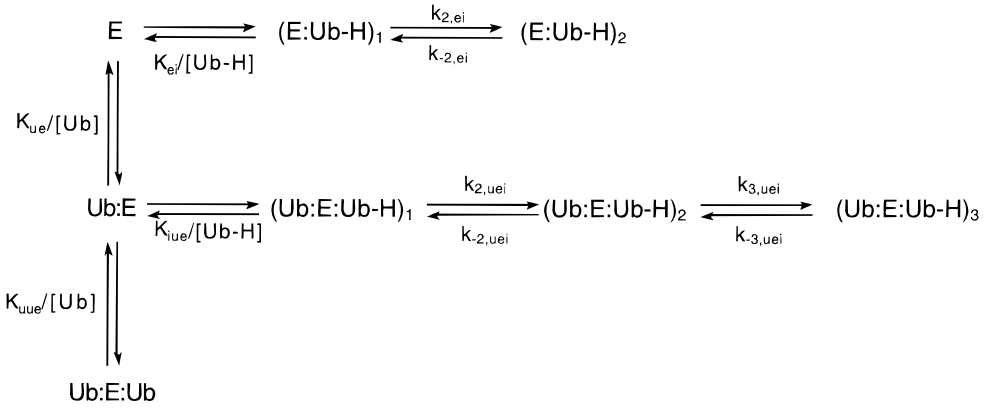

calculate $k_{-2,ei}$ from a rearranged version of eq 7 as 1.94×10^{-5} s^{-1}.

$$K_{ei}^* = K_{ei}\left(\frac{k_{-2ei}}{k_{2ei}}\right) \quad (7)$$

Triplicate experiments provide $k_{-2,ei} = (1.8 \pm 0.6) \times 10^{-5}$ s^{-1}.

To summarize, for the interaction of IPaseT with Ub-H we can calculate the following parameters: $K_{ei} = 260$ nM, $k_{2,ei} = 2.0 \times 10^{-3}$ s^{-1}, $k_{-2,ei} = 1.8 \times 10^{-5}$ s^{-1}, and $K_{ei}^* = 2.3$ nM.

Kinetics of Inhibition of Isopeptidase T by Ubiquitin Aldehyde in the Presence of Ubiquitin. We previously demonstrated that the peptidase activity of IPaseT is modulated by ubiquitin (Stein et al., 1995). Specifically, we found that while submicromolar concentrations of Ub activate IPaseT, higher concentrations are inhibitory. In the activation phase, k_c/K_m for the IPaseT-catalyzed hydrolysis of Z-Leu-Arg-Gly-Gly-AMC increases 50-fold relative to k_c/K_m for unactivated IPaseT. This activation occurs with a K_d for Ub of 0.1 μM. At higher concentrations, Ub is inhibitory and titrates k_c/K_m with a K_i of 3 μM. Given these results, it was of some interest to see if the interaction of Ub-H with IPaseT is also modulated by Ub.

To this end, we conducted progress curve experiments at Ub concentrations of 0.6 and 50 μM (see Figure 2 for examples). Progress curves at both of these Ub concentrations are characterized by a biphasic, exponential decay to steady-state velocities that equal zero. In experiments such as these, steady-state velocities of zero indicate that $[I] \geq 100K_i$. A subnanomolar inhibition constant was, in fact, confirmed in independent experiments where we demonstrate that at these concentrations of ubiquitin aldehyde, $K_i < 0.1$ nM (see below). Another mechanistically-significant feature of these progress curves is that they exhibit values of $v_{i,o}$ that are less than v_c.

Combined, these data suggest the general mechanism of Scheme 1 for the inhibition of IPaseT by Ub-H. According to this mechanism, free enzyme, E, can interact with Ub-H as described above or it can combine with a molecule of Ub to form Ub:E, the "Ub-activated" form of IPaseT. Ub:E then binds Ub-H, in a pre-equilibrium step, to form $(Ub:E:UbH)_1$ which then undergoes two sequential isomerization steps, first to $(Ub:E:UbH)_2$ and then onto $(Ub:E:UbH)_3$. Ub:E can also bind another molecule of Ub to form the "Ub-inhibited" species Ub:E:Ub.

Analysis of these progress curves begins with the determination of K_{iue}, the initial dissociation constant for inhibition of IPaseT by Ub-H. Equation 8 allows us to calculate K_{ieu}'.

$$K_{iue}' = \frac{[\text{Ub-H}]}{\frac{v_c}{v_{i,o}} - 1} - \frac{v_{i,o}}{v_c}[E] \quad (8)$$

where

$$K_{iue}' = K_{iue}\left(1 + \frac{[S]}{K_m} + \frac{[Ub]}{K_{uue}}\right) \quad (9)$$

Note that the magnitude of K_{iue}' depends both on substrate and ubiquitin concentration. In contrast to the condition of [Ub] = 0 where $[S] \ll K_m > 2$ mM, when the Ub concentration is 0.6 or 50 μM, $K_m = 170$ μM (Stein et al., 1995) and therefore competes for binding of Ub-H according to eq 9.

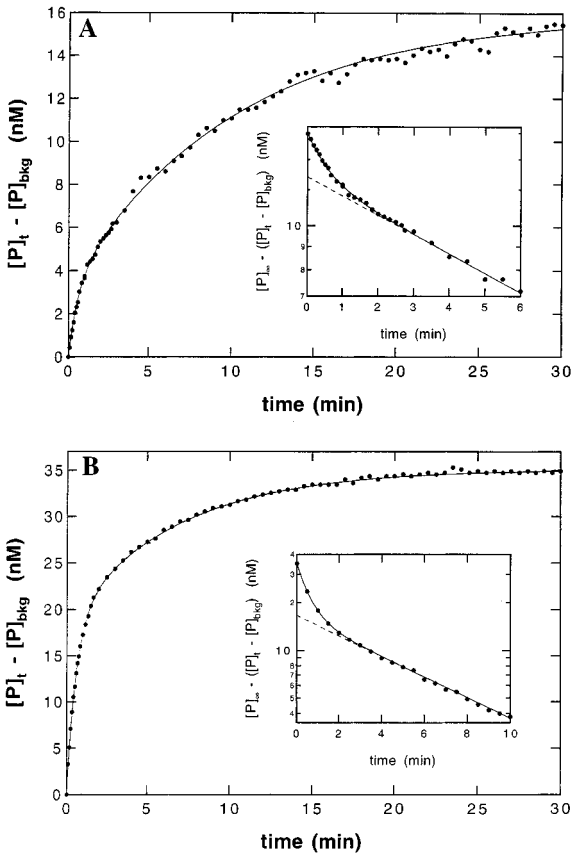

FIGURE 2: Progress curves for the inhibition of IPaseT by Ub-H in the presence Ub. Fluorescence intensity ($\lambda_{em} = 440$ nm, $\lambda_{ex} = 380$ nm) was recorded as a function of time for the IPaseT-catalyzed hydrolysis of Z-Leu-Arg-Gly-Gly-AMC in the presence of Ub-H, converted to AMC concentration, and plotted here as the difference between product AMC concentration at any time, t, and the background AMC concentration. The reaction was conducted at 25 °C in a pH 7.8 assay buffer containing 20 mM HEPES, 0.5 mM EDTA, 1 mg of ovalbumin/mL, and 10 mM DTT. For the two experiments of this figure, [IPaseT] = 0.05 μM, [Z-Leu-Arg-Gly-Gly-AMC] = 120 μM, and [Ub-H] = 0.22 μM. (A) [Ub] = 0.59 μM. The solid line through the data points was drawn with eq 10 and the best-fit parameters: $[P]_\infty = 16.9 \pm 0.2$ nM, $[P]_\alpha = 3.1 \pm 0.2$ nM, $k_\alpha = (27 \pm 5) \times 10^{-3}$ s^{-1}, $[P]_\beta = 13.8 \pm 0.2$ nM, and $k_\beta = (1.63 \pm 0.07) \times 10^{-3}$ s^{-1}. The inset is a semilogarithmic plot of $[P]_\infty - \Delta[P]$ vs time where $[P]_\infty$ is the product AMC concentration at the completion of the reaction and $\Delta[P]$ is the difference between product concentration at any time, t, and the background AMC concentration. (B) [Ub] = 50 μM. The solid line through the data points was drawn with eq 10 and the best-fit parameters: $[P]_\infty = 35.1 \pm 0.2$ nM, $[P]_\alpha = 18.4 \pm 0.2$ nM, $k_\alpha = (27.7 \pm 0.5) \times 10^{-3}$ s^{-1}, $[P]_\beta = 16.5 \pm 0.2$ nM, and $k_\beta = (2.49 \pm 0.04) \times 10^{-3}$ s^{-1}. The inset is again a semilogarithmic plot of $[P]_\infty - \Delta[P]$ vs time.

Values of K_{iue}' and K_{iue} along with the observed values of v_c and $v_{i,o}$ from which they were calculated are summarized in Table 1. The mechanism of Scheme 1 predicts that K_{iue} must be independent of Ub concentration and this is borne out in the identical calculated values of K_{iue}, 10.3 ± 1.3 and 11.5 ± 1.4, at Ub concentrations of 0.6 and 50 μM, respectively.

Having calculated the initial dissociation constant for the inhibition of IPaseT by Ub-H at Ub concentrations of 0.6 and 50 μM, we can now turn our attention to an analysis of the kinetics of inhibition. We found that the biphasic

Table 1: Initial Dissociation Constants for the Inhibition of IPaseT by Ub-H

[Ub] (μM)	expt no.	v_c (nM/s)	$v_{i,o}$ (nM/s)	K_{iue}' [a] (nM)	K_{iue} [b] (nM)
0.6	1	1.34	0.12	17	8.9
	2	1.54	0.16	20	10.5
	3	1.71	0.20	22	11.5
				20 ± 3	10.3 ± 1.3
50	1	0.71	0.39	230	12.6
	2	0.79	0.53	182	9.9
	3	0.81	0.43	221	12.1
				210 ± 25	11.5 ± 1.4

[a] K_{iue}' was calculated according to eq 8. [b] K_{iue} was calculated according to eq 9.

Scheme 2: Simplified Mechanism of Inhibition of IPaseT by Ub-H

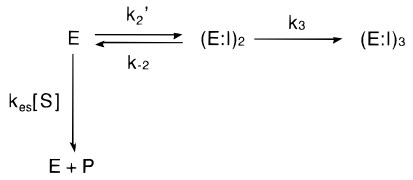

progress curves that were collected (see Figure 2 for examples) can be satisfactorily fit to the simple double-exponential expression of eq 10.

$$[P]_t = [P]_\infty(1 - [P]_\alpha e^{-k_\alpha t} - [P]_\beta e^{-k_\beta t}) \quad (10)$$

However, this analysis does not directly provide mechanistic parameters. The mechanistic parameters of Scheme 1 are related to the empirical parameters, k_α and k_β, in a complex manner (Johnson, 1986). To calculate estimates for the mechanistic parameters of Scheme 1 we employed a method of numerical analysis in which the progress curves were fit to the following rate equations corresponding to the simplified mechanism of Scheme 2.

$$\frac{d[P]}{dt} = k_{es}[S][E] \quad (11)$$

$$\frac{d[E]}{dt} = -k_2'[E] + k_{-2}[(E:I)_2] \quad (12)$$

$$\frac{d[(EI)_2]}{dt} = k_2'[E] - k_{-2}[(E:I)_2] - k_3[(E:I)_2] \quad (13)$$

The parameters of this simplified mechanism correspond to the mechanism of Scheme 1 according to the following equalities:

$$k_2' = k_{2,uei}\frac{[Ub\text{-}H]}{[Ub\text{-}H] + K_{iue}} \quad (14)$$

$$k_{-2} = k_{-2,uei} \quad (15)$$

$$k_3 = k_{3,uei} \quad (16)$$

where E is IPaseT, I is Ub-H, $(E:I)_2$ is $(Ub:E:Ub\text{-}H)_2$, and $(E:I)_3$ is $(Ub:E:Ub\text{-}H)_3$.

The fitting was accomplished using a program designed to replace the function evaluations of a standard nonlinear least-squares method with numerical integration.[2] This fitting procedure directly provides least-squares estimates of the actual rate constants in the mechanistic scheme. The calculated parameters are summarized in Table 2.[3]

Table 2: Mechanistic Rate Constants for the Inhibition of IPaseT by Ub-H[a]

[Ub] (μM)	expt no.	$k_{2,uei}$ (10^{-3} s^{-1})	$k_{-2,uei}$ (10^{-3} s^{-1})	$k_{3,uei}$ (10^{-3} s^{-1})
0.6	1	8.0 ± 0.3	1.39 ± 0.07	1.29 ± 0.02
	2	23.5 ± 2.1	2.58 ± 0.15	1.05 ± 0.05
	3	16.2 ± 0.4	1.00 ± 0.02	0.76 ± 0.01
		16 ± 8	1.7 ± 0.8	1.0 ± 0.3
50	1	23.7 ± 0.5	1.64 ± 0.04	2.65 ± 0.05
	2	16.2 ± 0.2	0.86 ± 0.02	1.42 ± 0.03
	3	17.4 ± 0.2	0.98 ± 0.02	1.37 ± 0.02
		19 ± 4	1.2 ± 0.4	1.8 ± 0.7

[a] See text for details of analysis.

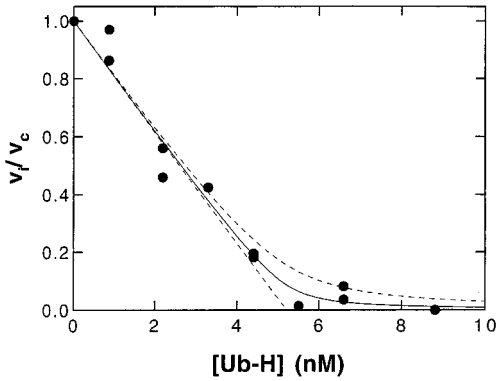

FIGURE 3: Titration of IPaseT with Ub-H. In this experiment, various concentrations of Ub-H were incubated with 5 nM IPaseT for three hours at 25 °C in assay buffer containing 0.6 μM Ub. Residual peptidase activity was measured at the end of the incubation and plotted here as v_i/v_c vs time. The solid line through the data was drawn using eq 17 and the best-fit parameters: [IPaseT] = 5.2 ± 0.4 nM and $K_{i,app} = 43 \pm 71$ pM. The dashed line below the solid was drawn using eq 17 and the parameters [IPaseT] = 5.2 nM and $K_{i,app} = 1$ pM, while the dashed line above the solid line was drawn using eq 17 and the parameters [IPaseT] = 5.2 nM and $K_{i,app} = 150$ pM.

Dissociation Constant for the Inhibition of Ubiquitin-Activated Isopeptidase T by Ubiquitin Aldehyde. To determine the steady-state dissociation constant for the inhibition of Ub-activated IPaseT by Ub-H, we conducted enzyme titration experiments in which residual activity is measured for enzyme reaction solutions in which $[I]_o \approx [E]_o \gg K_i$. Data from two independent experiments are plotted in Figure 3 as relative residual activity vs Ub-H concentration. To determine the K_i value, we fit the data to the expression of eq 17 for tight-binding inhibition (Morrison & Walsh, 1988; Szedlacsek & Duggleby, 1995).

$$\frac{v_{i,s}}{v_c} = \frac{1}{2[E]_o}\{([E]_o - [I]_o - K_i) + \sqrt{([I]_o + K_i - [E]_o)^2 + 4K_i[E]_o}\} \quad (17)$$

This expression provides estimates for both the steady-state

[2] Subroutines lmfdif1 and lsode and supporting routines obtained from http://www.netlib.org were used in a Fortran program to carry out the least-squares fits. This type of analysis has been described by Zimmerle and Frieden (1989).

[3] In this analysis, the calculated value of $k_{2,uei}'$ very closely approximates $k_{2,uei}$ since in these experiments [Ub-H] = 220 nM $\gg$ $K_{iue} = 10$ nM, $k_{2uei}' = k_{2uei}$.

Scheme 3: Mechanistic Kinetic Parameters for Inhibition of Isopeptidase T by Uniquitin Aldehyde

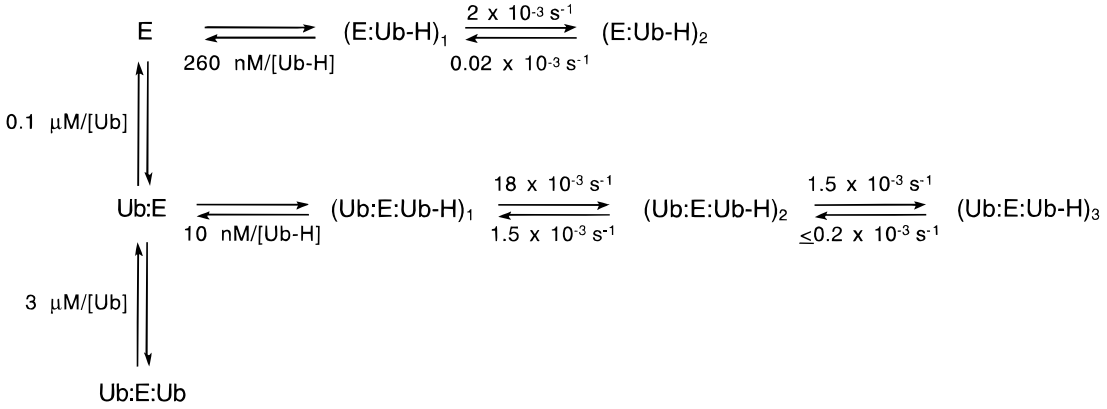

K_i and the enzyme concentration, which are 0.04 ± 0.08 and 5.2 ± 0.4 nM, respectively. The enzyme concentration derived from this exercise is identical to the nominal concentration of IPaseT that was used in these experiments. The K_i value is associated with such a large error that all we can conclude is that $K_i \leq 0.1$ nM.

K_{iue}*, the final, steady-state dissociation constant, is related to the mechanistic parameters of Scheme 1 as shown in eq 18.

$$K_{iue}^* = K_{iue}\left(\frac{k_{-2,uei}}{k_{2,uei}}\right)\left(\frac{k_{-3,uei}}{k_{3,uei}}\right) \tag{18}$$

This expression together with the estimate of K_{iue}* and the other mechanistic parameters allow us to calculate $k_{-3,uei}$ as 0.2×10^{-3} s^{-1}. These values are all summarized in Scheme 3.

DISCUSSION

In this paper, we report the first kinetic characterization of the inhibition of a ubiquitin C-terminal hydrolase by ubiquitin aldehyde. We find that Ub-H is a potent, time-dependent inhibitor of isopeptidase T and that the inhibition is modulated by Ub. In this section, we comment on three key findings: (i) IPaseT binds Ub-H with much higher affinity than it binds Ub. (ii) Ub increases the binding affinity of IPaseT for Ub-H. (iii) The kinetic mechanism of inhibition of IPaseT by Ub-H is complex and proceeds through several kinetically-distinguishable intermediates.

IPaseT Binds Ub-H with Much Higher Affinity Than It Binds Ub. We estimate the steady-state dissociation constant for inhibition of Ub-activated IPaseT by Ub-H, K_{iue}*, to be less than or equal to 0.1 nM. Before we analyze and interpret this value in any detail we should first consider that this inhibition constant does not accurately reflect the affinity of IPaseT for Ub-H, but rather this value must be corrected for the hydration of Ub-H (Lewis & Wolfenden, 1977). This correction is given in eq 19.

$$(K_i)_{corr} = \frac{K_i}{1 + K_{hyd}[H_2O]} \tag{19}$$

where K_i is the observed inhibition constant and

$$K_{hyd} = \frac{[\text{hydrate}]}{[\text{aldehyde}][H_2O]} \tag{20}$$

Since $K_{hyd}[H_2O]$ is around 10 for aldehydes of general structure R-NH-CH_2-C(O)H (Lewis & Wofenden, 1977a,b), $(K_{iue}^*)_{corr}$ is less than 10 pM. This value reflects the true affinity of IPaseT for Ub-H.

On the basis of these calculations we see that the binding affinity of Ub-activated IPaseT for Ub-H is at least 300 000 times greater than its affinity for Ub. To understand this dramatic difference in binding energy ($\Delta G = 7.6$ kcal/mol) we need to consider how Ub-activated IPaseT (Ub:E of Scheme 1) interacts with Ub-H and with Ub and the forces that stabilize the two resultant complexes, Ub:E:Ub-H and Ub:E:Ub, respectively.

The binding of Ub to Ub:E is mediated primarily through interactions of the enzyme with the bulk of the Ub molecule and has little to do with the C-terminus of Ub. This is evidenced by the nearly identical values of K_{uue} for Ub and des-Gly^{75}Gly^{76}-Ub of 3 and 5 μM, respectively (Stein et al., 1995). This implies that the 300 000-fold increase in binding affinity that is observed for Ub-H must be due to its C-terminal aldehydic functionality and strongly suggests that Ub-H forms a hemithioacetal with the active site Cys residue of IPaseT. This mechanism of inhibition is identical to the mechanism of inhibition of Cys proteases by peptide aldehydes (Lewis & Wofenden, 1977a,b). For these enzymes, and presumably also for IPaseT, tight binding of aldehyde analogs of specific substrates derives from the resemblance of the hemithioacetals to tetrahedral transition states that occur along the enzyme-catalyzed reaction pathway. Thus, Ub-H is a transition-state analog inhibitor of IPaseT and probably other UCH's (Mayer & Wilkinson, 1989).

Ub Increases the Binding Affinity of IPaseT for Ub-H. Previously reported studies from our laboratory revealed that while submicromolar concentrations of Ub activate IPaseT, higher concentrations of Ub inhibit IPaseT (Stein et al., 1995). To explain these observations, we proposed a structural model for IPaseT involving two binding sites for Ub. According to this model, the two sites are adjacent to one another and are the extended active site that binds two Ub moieties of a polyUb chain for isopeptide bond hydrolysis. The "activation site" binds the Ub molecule that donates Lys^{48} to the isopeptide bond in polyUb substrates and binds monomeric Ub with a K_d of 0.1 μM. The "inhibition site" is adjacent and binds the Ub molecule that donates the C-terminal Gly^{76} to the isopeptide bond of the polyUb substrate. This site binds monomeric Ub with a K_i of 3 μM.

On the basis of these observations, one might predict that occupancy of the "activation site" by Ub would also be

Scheme 4: Thermodynamic Cycle for the Modulation of Binding Affinity of Isopeptidase T by Ubiquitin

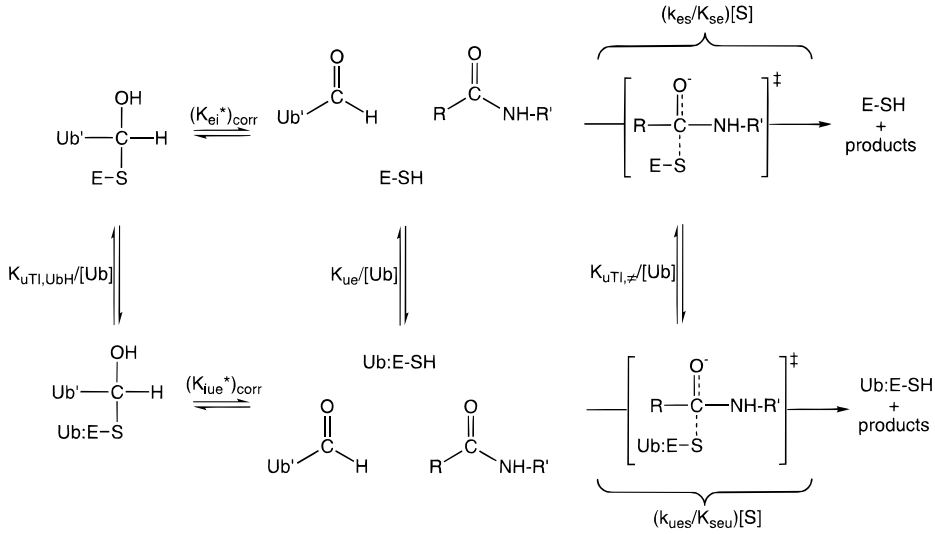

Table 3: Ubiquitin-Dependent Modulation of Inhibitor and Transition State Binding

	kinetic parameter	K_{ux} (nM)[a]
Ub-H		
$(K_{ei}^*)_{corr}$ (pM)	230	<4.4
$(K_{iue}^*)_{corr}$ (pM)	<10	
Z-RGG-AMC[b]		
k_{es}/K_{se} (M^{-1} s^{-1})	1	12.5
k_{ues}/K_{seu} (M^{-1} s^{-1})	8	
Z-LRGG-AMC[a]		
k_{es}/K_{se} (M^{-1} s^{-1})	30	5.9
k_{ues}/K_{seu} (M^{-1} s^{-1})	508	
Z-RLRGG-AMC[a]		
k_{es}/K_{se} (M^{-1} s^{-1})	121	6.7
k_{ues}/K_{seu} (M^{-1} s^{-1})	1810	

[a] K_{ux} is the Ub dissociation constant for either the hemithioacetal inhibition species or the catalytic transition state. For inhibition by Ub-H, $K_{ux} = K_{ue}[(K_{iue}^*)_{corr}/(K_{ei}^*)_{corr}]$, while for substrate hydrolysis, $K_{ux} = K_{ue}[(k_{es}/K_{se})/(k_{ues}/K_{seu})]$. K_{ue} = 100 nM (Stein et al., 1995). [b] k_{es}/K_{se} and k_{ues}/K_{seu} are apparent k_c/K_m values determined at 0 and 0.5 μM Ub, respectively (Stein et al., 1995).

accompanied by an increase in binding affinity of IPaseT for Ub-H, if Ub-H is a transition state analog inhibitor of IPaseT, as we argued in the previous section. And, in fact, this prediction is borne out by experiment. As summarized in Table 3, when Ub concentration is increased from 0 to 0.6 μM, $(K_i^*)_{corr}$ for inhibition of IPaseT by Ub-H decreases from 230 pM to a value less than 10 pM and parallels the increase in k_c/K_m that is observed for IPaseT-catalyzed hydrolysis of peptide−AMC substrates.

In Scheme 4, we detail the thermodynamic basis for this prediction. This scheme posits a single, unifying mechanism for the Ub-dependent modulation of the affinity of IPaseT for tetrahedral species that are encountered either during catalysis or inhibition. In the catalytic cycle, we see that the following must hold:

$$\frac{k_{ues}/K_{seu}}{k_{es}/K_{se}} = \frac{K_{ue}}{K_{uTI,\ddagger}} \qquad (21)$$

Activation of IPaseT means, of course, that k_{ues}/K_{seu} is greater than k_{es}/K_{se} and, thus, that the catalytic transition state binds Ub with greater affinity than the reactant state; that is, $K_{uTI}^{\ddagger}$ is less than K_{ue}.

Table 4: Summary of Operational Kinetic Constants for the Inhibition of IPaseT by Ub-H

[Ub] (μM)	k_{on} [a] (10^3 M^{-1} s^{-1})	k_{off} [b] (10^{-5} s^{-1})	K_i^* [c] (nM)
0	8	2	2.3
0.6	1800	<20	<0.1

[a] At [Ub] = 0, $k_{on} = k_{2ei}/K_{ei}$, while at [Ub] = 0.6, $k_{on} = [k_{3uei}/K_{iu}(k_{-2uei}/k_{2uei})]$. These values are uncorrected for hydration. [b] At [Ub] = 0, $k_{off} = k_{-2ei}$, while at [Ub] = 0.6, $k_{off} = k_{-3uei}$. [c] Observed, steady-state dissociation constants, uncorrected for hydration. Measured as described in text at the two concentrations of Ub.

Likewise, in the inhibition cycle:

$$\frac{(K_{ei}^*)_{corr}}{(K_{iue}^*)_{corr}} = \frac{K_{ue}}{K_{uTI,UbH}} \qquad (22)$$

This means that the observed increase in binding affinity of IPaseT for Ub-H in the presence of Ub [i.e., $(K_{iue}^*)_{corr} < (K_{ei}^*)_{corr}$] results from tighter binding of Ub by the hemithioacetal than by free IPaseT (i.e., $K_{uTI,UbH} < K_{ue}$).

The unifying theme that emerges here is that binding of Ub either to catalytic transition states or to tetrahedral inhibition intermediates liberates more free energy than binding of Ub to the reactant state of IPaseT. This is apparent when we compare the K_{ux} values of Table 3 with the K_{ue} of 100 nM. K_{ux} is the equilibrium constant for dissociation of Ub from either the hemithioacetal inhibition intermediate or from the tetrahedral catalytic transition state (see Scheme 4). The average value for K_{ux} is 8 nM and is 12-fold less than K_{ue}. IPaseT can utilize the energy that is derived from this tighter binding to stabilize both tetrahedral species. The overall effect is a Ub-induced increase in catalytic efficiency or inhibitory potency.

Inhibition of IPaseT by Ub-H Proceeds through Several Intermediates. In the absence of Ub, Ub-H interacts with IPaseT through a two-step mechanism to form the final, stable complex that accumulates in the steady-state. The first step is rapid and governed by a dissociation constant, K_{ei}, that is equal to 260 nM. The overall k_{on} for the inhibition of IPaseT by Ub-H is 8 mM^{-1} s^{-1}, and k_{off} for the reaction is 2×10^{-5} s^{-1} (see Table 4). In contrast, concentrations of Ub that activate IPaseT cause a change in kinetic mechanism

to one involving three steps. At [Ub] = 0.6 μM, the first step is rapid and characterized by a dissociation constant equal to 10 nM (see Scheme III). The subsequent two steps are progressively slower with relaxation times of 0.5 and 10 min, respectively (see Figure 2A). The overall k_{on} is 1800 mM^{-1} s^{-1} and k_{off} is $<20 \times 10^{-5}$ s^{-1} (see Table 4).

While we have been able to elucidate the kinetic mechanism of inhibition of IPaseT by Ub-H and estimate the kinetic parameters for this mechanism (see Scheme 3), we are not able to provide any structural insight into the intermediates of this mechanism. Although we can say with some certainty that both $(E:Ub\text{-}H)_2$ and $(Ub:E:Ub\text{-}H)_3$ represent species in which Ub-H has formed a hemithioacetal with the active site Cys of IPaseT, we really cannot comment on the structures of $(E:Ub\text{-}H)_1$, $(Ub:E:Ub\text{-}H)_1$, or $(Ub:E:Ub\text{-}H)_2$. One can imagine that $(E:Ub\text{-}H)_1$ is a simple "Michaelis complex" of IPaseT and Ub-H which slowly converts to the hemithioacetal $(E:Ub\text{-}H)_2$. Equally possible is that hemithioacetal formation occurs rapidly to produce $(E:Ub\text{-}H)_1$ which then undergoes a slow conformational isomerization to form the highly stabilized hemithioacetal species $(E:Ub\text{-}H)_2$. Similar mechanistic scenarios can be imagined for how Ub:E combines with Ub-H to finally form the stable hemithioacetal $(Ub:E:Ub\text{-}H)_3$. However, at this time we cannot offer experimental support for any of these mechanistic hypotheses.

REFERENCES

Chen, Z., & Pickart, C. M. (1990) *J. Biol. Chem. 265*, 21835−21842.

Ciechanover, A. (1994) *Cell 79*, 13−21.

Dunten, R. L., & Cohen, R. E. (1989) *J. Biol. Chem. 264*, 16739−16747.

Finley, D., & Chau, V. (1991) *Annu. Rev. Cell. Biol. 7*, 25−69.

Goldberg, A. L., & Mitch, W. (1996) *N. Eng. J. Med.* (in press).

Greco, W. R., & Hakala, M. T. (1979) *J. Biol. Chem. 254*, 12104−12109.

Hadar, T., Warms, J. V. B., Rose, I. A., & Hershko, A. (1992) *J. Biol. Chem. 267*, 719−727.

Hershko, A., & Rose, I. A. (1987) *Proc. Natl. Acad. Sci. U.S.A. 84*, 1829−1833.

Hochstrasser, M. (1995) *Curr. Opin. Biol. 7*, 215−223.

Johnson, K. A. (1986) *Methods Enzymol. 134*, 677−705.

Lewis, C. A., & Wofenden, R. (1977a) *Biochemistry 16*, 4886−4890.

Lewis, C. A., & Wolfenden, R. (1977b) *Biochemistry 16*, 4890−4895.

Mayer, A. N., & Wilkinson, K. D. (1989) *Biochemistry 28*, 166−172.

Morrison, J. F., & Walsh, C. T. (1988) *Adv. Enzymol. 61*, 201−301.

Pickart, C. M., & Rose, I. A. (1985) *J. Biol. Chem. 260*, 7903−7910.

Pickart, C. M., & Rose, I. A. (1986) *J. Biol. Chem. 261*, 10210−10217.

Stein, R. L., Chen, Z., & Melandri, F. (1995) *Biochemistry 34*, 12616−12623.

Szedlacsek, S. E., & Duggleby, R. G. (1995) *Methods Enzymol. 249*, 144−180.

Wilkinson, K. D. (1995) *Annu. Rev. Nutr. 15*, 161−189.

Wilkinson, K. D., Cox, M. J., Mayer, A. N., & Frey, T. (1986) *Biochemistry 25*, 6644−6649.

Wilkinson, K. D., Tashayev, V. L., O'Conner, L. B., Larsen, C. N., Kasperek, E., & Pickart, C. M. (1995) *Biochemistry 34*, 14535−14546.

Williams, J. W., & Morrison, J. F. (1979) *Methods Enzymol. 63*, 437−467.

Zimmerle, C. T., & Frieden, C. (1989) *Biochem. J. 258*, 381−387.

BI9612935